JOURNAL OF MATERIALS SCIENCE 21 (1986) 1051–1056

A mechanism for ductile crack growth in epoxy polymers

A. J. KINLOCH
Department of Mechanical Engineering, Imperial College of Science and Technology, Exhibition Road, London SW7 2BX, UK

D. G. GILBERT*
Engineering Department, University of Cambridge, Trumpington Street, Cambridge CB2 1PZ, UK

S. J. SHAW
Ministry of Defence (PE), RARDE, Waltham Abbey, Essex EN9 1BP, UK

It has been previously shown that at relatively high test temperatures/slow test rates crack propagation in thermosetting epoxy polymers occurs in a stable ductile manner. The present paper proposes a mechanism for this type of crack growth based upon a meniscus instability model which both qualitatively and quantitatively accounts for the experimental observations.

1. Introduction

The use of adhesives and continuous-fibre reinforced-plastics in structural engineering applications has increased markedly over the last few years and these materials largely employ thermosetting epoxy polymers, either as the basis for the structural adhesive compositions or as the matrix for glass-, polyaramid- and carbon-fibre composites. Both unmodified epoxy polymers and multiphase, rubber-toughened epoxies are used in such applications, with the latter polymers increasingly finding favour due to their improved crack resistance [1].

Previous work [1–6] has investigated the fracture behaviour of unmodified and rubber-modified epoxy polymers and clearly demonstrated that both the fracture toughness, K_{Ic}, and manner in which the crack propagates through the specimen are highly dependent upon the test temperature and rate of test. Three types of crack growth behaviour have been identified. At the lowest temperatures/fastest rates, K_{Ic} is low and the crack propagates in a stable, brittle manner. At intermediate temperatures and loading rates, K_{Ic} rises and brittle, unstable (stick-slip) crack growth occurs. Finally, at the highest test temperatures/slowest rates the value of K_{Ic} is relatively high and the crack propagates in a stable ductile manner.

The purpose of the present paper is to describe ductile crack growth in epoxy polymers. A mechanism is proposed for this type of crack growth which explains, both qualitatively and quantitatively, the experimental observations.

2. Experimental details

2.1. The materials

The epoxy resin employed was derived from the reaction of bisphenol A and epichlorhydrin and was largely composed of the diglycidyl ether of bisphenol A (DGEBA). The curing agent used was piperidine.

The rubber used to prepare the multiphase, rubber-modified epoxy polymers was a carboxyl-terminated, random copolymer of butadiene and acrylonitrile (CTNB rubber: carboxyl content 2.37 wt/wt %; acrylonitrile content 18 wt/wt %; molar mass rubber 3500 g mol^{-1}).

The formulations of the epoxy polymer are shown in Table I.

To prepare sheets of the rubber-modified epoxy the CTBN rubber was added to the epoxy resin and hand-mixed for approximately 5 to 10 min. This mixture was then heated to 65 ± 5° C in a water bath and mixed for 5 min using an electric stirrer and then degassed in a vacuum oven at 60° C until frothing stopped. When the mixture had cooled to below 30° C the piperidine was mixed in gently to minimize air entrapment. The rubber–epoxy mixture was then poured into a preheated mould, cured at 120° C for 16 h and allowed to cool slowly. The unmodified epoxy was prepared in the same manner without the addition of rubber.

2.2. Mechanical properties

Since the epoxy polymers under study fracture when tested in uniaxial tension prior to plastic yielding, their yield behaviour was examined by testing in uniaxial compression. Cylindrical rods of the cured epoxies were cast as described above, and then machined to give test specimens with a height-to-diameter ratio of nominally 2:1. The specimens were deformed in a compression cage between polished steel plates lubricated with molybdenum disulphide grease. A constant displacement rate, $\dot{y}$, was used for each test and this was converted to a strain rate, $\dot{e}$. The nominal strain, e, was determined from the crosshead displacement corrected for the machine deflection using a steel blank. The load, P, was measured from the load–displacement record and converted into a true stress,

* *Present address*: BP Research Centre, Sunbury-on-Thames, Middlesex, UK.

0022–2461/86 $03.00 + .12

TABLE I Formulations of epoxy materials

	Unmodified epoxy (phr)*	Rubber-modified epoxy (phr)
DGEBA epoxy resin	100	100
Piperidine	5	5
CTBN rubber	—	15

*phr = parts per hundred by weight.

σ, using the initial specimen cross-sectional area, A_0, in the equation

$$\sigma = \frac{P}{A_0}(1 - e) \quad (1)$$

which assumes constant-volume deformation. The true compressive modulus, E, true compressive yield stress, σ_{yc}, and the yield strain, e_y, were also determined.

2.3. Fracture studies

The fracture behaviour of the epoxy polymers was examined by a fracture mechanics approach. The fracture toughness, K_{Ic}, for the initiation of crack growth was determined using compact-tension specimens [1, 2]. Essentially, a sharp crack was inserted in the specimen which was then mounted in a tensile testing machine and loaded at a constant displacement rate, $\dot{y}$. The associated load versus displacement was recorded and the value of K_{Ic} was calculated from

$$K_{Ic} = \frac{P_c Q}{b w^{1/2}} \quad (2)$$

where P_c is the load at crack initiation, a the crack length, Q a geometry factor $= 29.6\ (a/w)^{1/2} - 185.5\ (a/w)^{3/2} + 655.7\ (a/w)^{5/2} - 1017\ (a/w)^{7/2} + 638.9\ (a/w)^{9/2}$, w the width of the specimen, and b the thickness of the specimen.

2.4. Fractography

The fracture surfaces were examined in a scanning electron microscope (Cambridge Instruments) at a relatively low beam current and accelerating voltage of approximately 175 mA and 20 kV, respectively. Prior to examination the surfaces were coated with a thin evaporated layer of gold in order to improve conductivity and prevent charging effects on the surface of the specimens.

3. Fracture toughness and type of crack growth

3.1. Effect of test temperature and rate

The effect of test temperature on the measured value of fracture toughness, K_{Ic}, is shown in Fig. 1. As may be seen, the values of K_{Ic} for the rubber-modified epoxy are appreciably higher than for the unmodified epoxy and more dependent upon the test conditions. The reasons for these observations have been discussed previously [2, 3] but essentially arise from a greater extent of energy dissipating deformations occurring in the vicinity of the tip in the multiphase, rubber-modified material. The deformation processes are (i) microvoiding in the rubbery particle, or at the particle/matrix interface, and (ii) multiple, but localized shear yielding in the matrix initiated by the stress concentrations associated with the rubbery particles.

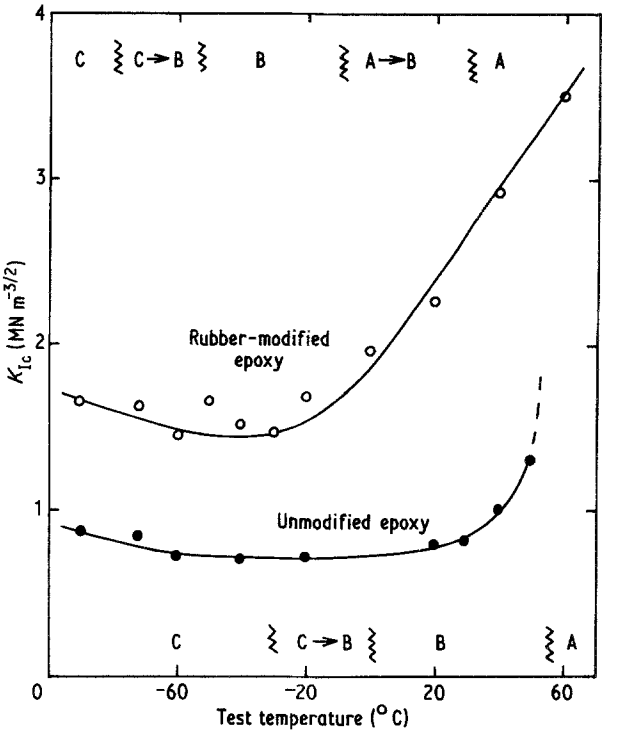

Figure 1 Fracture toughness, K_{Ic}, at the onset of crack growth as a function of test temperature for the unmodified and rubber-modified epoxies. The displacement rate, $\dot{y}$, is 1.67×10^{-5} m sec^{-1}. Types of crack growth are: type A, ductile stable crack growth; type B, brittle unstable crack growth; type C; brittle stable crack growth; type C → B or A → B indicates that some slow crack growth (of type C or A) preceded brittle unstable crack growth (type B).

Also shown in Fig. 1 are the types of crack growth observed over the wide range of test temperatures studied. With both materials three basic types of crack growth may be identified as given below.

1. Brittle stable crack growth (type C) – here the crack grows in a steady controlled manner with the rate of crack propagation being dependent upon the crosshead displacement rate of the testing machine. It is generally favoured by low test temperatures and/or very high displacement rates. Under these conditions the yield stress is relatively high (see [3] and the discussion below) and the extent of plastic deformation at the crack tip is therefore limited and the crack tip relatively sharp. Hence, the value of K_{Ic} for crack growth is comparatively low and almost independent of rate and temperature.

2. Brittle unstable crack growth (type B) – this type of crack growth is still basically brittle in nature but the crack propagates intermittently in a stick/slip manner. Thus initiation and arrest values of K_{Ic} may be determined. This type of crack growth is favoured by lower test rates and higher test temperatures compared to the conditions under which brittle stable crack growth (type C) is observed. It arises because under these conditions the yield stress of the material decreases and the extent of crack tip deformation and blunting becomes more severe. This leads to K_{Ic} (initiation) being greater than K_{Ic} (propagating crack), and the relatively large amount of stored elastic energy in the specimen at the onset of crack growth results in fast unstable crack

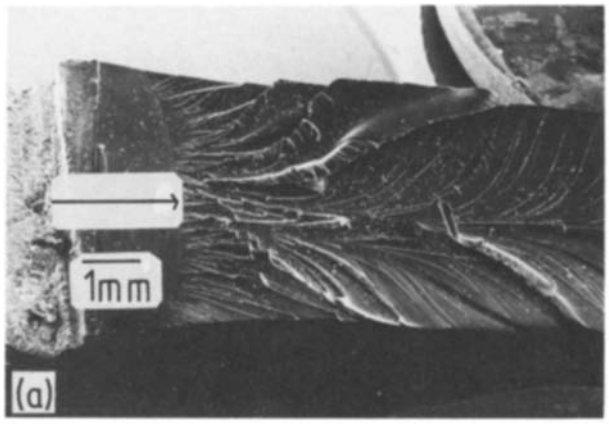

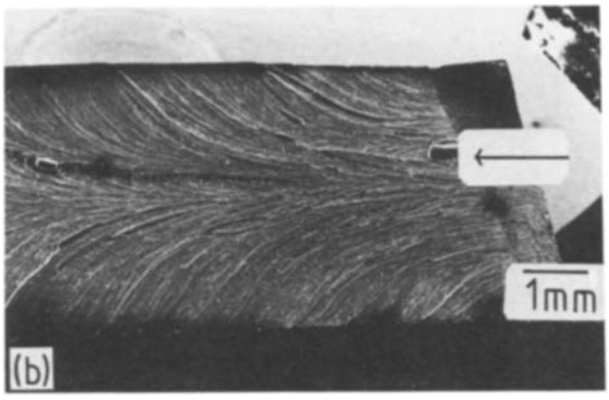

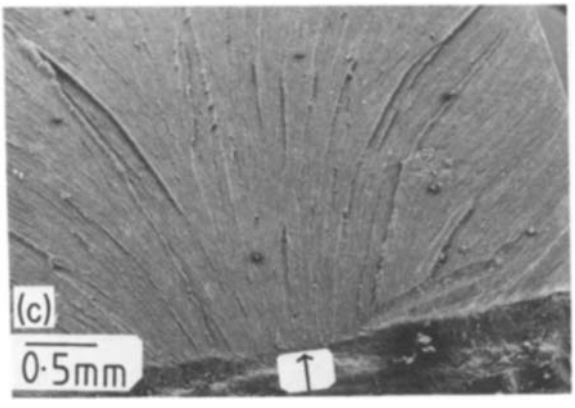

Figure 2 Scanning electron micrographs of fracture surfaces resulting from ductile stable (type A) crack growth at a test temperature of 60° C and rate, $\dot{y}$, of 1.67×10^{-5} m sec^{-1}. (a) Unmodified epoxy. (b) and (c) Rubber-modified epoxy. (Arrow indicates length of initial, starter crack and direction of main crack growth.)

propagation until the energy supply is insufficient to sustain crack growth and crack arrest occurs.

3. Ductile stable crack growth (type A) – at the highest test temperatures stable crack propagation is again observed. However, unlike the brittle stable crack growth discussed in (1), a relatively high value of K_{Ic} is now required. Under these test conditions the yield stress of the polymer is relatively very low and extensive plastic deformation and blunting occurs at the crack tip. This leads to a highly ductile fracture and this type of crack growth, and the responsible mechanisms, are studied in more detail below.

3.2. Ductile stable crack growth

Scanning electron micrographs of the fracture surfaces of unmodified and rubber-modified epoxies where ductile stable crack growth (type A) has occurred are shown in Fig. 2. As may be seen, these micrographs are at relatively low magnifications and under these circumstances the two epoxy polymers have a somewhat similar appearance. In both materials the fracture surfaces are very rough, torn-like in character and contain many river markings and finger-like furrows. At slightly higher magnification the finger-like furrows can be even more clearly seen extending from the advancing crack front. These finger-like markings veer away from the centre-line towards the edges of the specimen which is probably associated with edge effects, i.e. the centre of the specimen is in a state of plane-strain (triaxial tensile stresses) whilst towards the edges this condition is relaxed and a state of plane-stress (biaxial tensile stresses) exists. Other epoxy polymers have been found [4, 5] to show similar behaviour at relatively high test temperatures/low test rates.

For the unmodified epoxy, scanning electron micrographs taken at higher magnifications do not reveal any further features of interest. However, for the rubber-modified epoxy polymer further features are revealed and a higher magnification scanning electron micrograph of the fracture surface is shown in Fig. 3. The finger-like furrows are again clearly visible, but this micrograph also shows the appearance of a large number of holes. Many of the holes are relatively deep, apparently containing little rubber but it has been shown [2] that most of the rubber is still in the holes, as a lining on the inside. It appears that the triaxial tensile stresses ahead of the crack cause microvoiding in the rubbery particles, or debonding at the particle/matrix interface. The micrograph shown in Fig. 4 clearly shows this microvoiding and supports the former suggestion. The failed particles appear as holes both because the triaxial stress that exists initially in the particle from the difference in thermal expansion between the rubber and the epoxy causes the rubber to contract and because plastic deformation of the matrix increases the size of the cavity. (It is the microvoiding of the rubbery particles which causes the stress-whitening of the fracture surfaces of the rubber-modified epoxy during ductile crack growth. Obviously, this effect is absent in the unmodified epoxy polymers.)

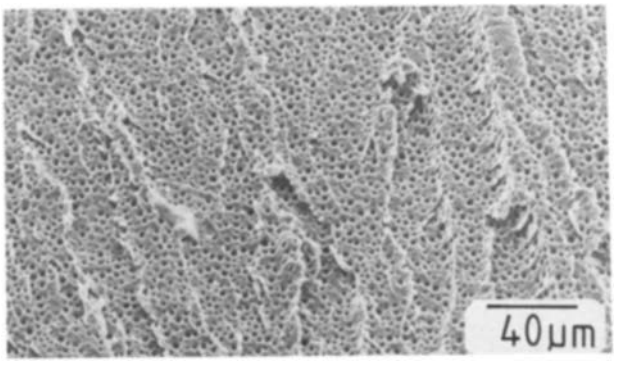

Figure 3 Scanning electron micrograph of fracture surface of rubber-modified epoxy resulting from ductile stable crack growth at a test temperature of 60° C and a rate, $\dot{y}$, of 1.67×10^{-5} m sec^{-1}.

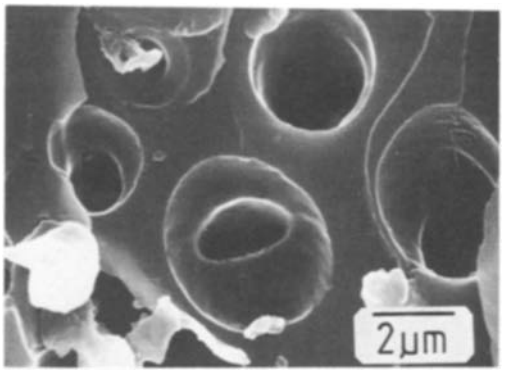

Figure 4 Scanning electron micrograph of fracture surface of rubber-modified epoxy showing voided rubbery particles. (Same specimen and test conditions as in Fig. 3.)

4. Mechanism for ductile crack growth

4.1. Introduction

In two classic papers, Taylor [7] and Saffman and Taylor [8] considered the advance of a meniscus between a less-dense and more-dense fluid flowing through a channel. They demonstrated that under certain circumstances the smooth meniscus breaks-up into a series of fingers of the less-dense fluid advancing into the more-dense fluid, ahead of the general interface front. More recently several groups of workers [9–13] have invoked this mechanism to explain finger-like growth in a variety of liquids, metallic solid and craze growth in thermoplastic, glassy polymers.

4.2. Theory

To model ductile crack growth in the epoxy polymers by the meniscus instability mechanism one may consider the advance of a meniscus (the crack front) through a non-Newtonian fluid (the plastic zone ahead of the advancing crack) between two rigid plates (the elastically deformed polymer outside the zone).

The above model is shown schematically in Fig. 5, and the first step is to suppose that the crack front suffers a small sinusoidal perturbation, i.e.

$$x = a \sin\left(\frac{2\pi z}{\lambda}\right) \tag{3}$$

where a is the amplitude and λ is the wavelength of the perturbation and z is defined in Fig. 5. This obviously introduces a new curvature to the crack front, and the maximum value, R, of the advancing perturbation is given by

$$\frac{1}{R} = \frac{d^2x}{dz^2} = \frac{4\pi^2 a}{\lambda^2} \tag{4}$$

Now there will be a gradient of local hydrostatic tensile stress, dp/dx, ahead of the crack tip; where $p = I_1/3$ and I_1 is the first stress invariant. This gradient of local hydrostatic tensile stress will tend to increase the amplitude of the perturbation. However, the perturbation will not grow, so leading to the development of a "finger", unless the increment of hydrostatic tensile stress, $(dp/dx)_0 a$ exceeds that required to produce the new radius of curvature, G_0/R; where G_0 is the intrinsic fracture energy, i.e. the

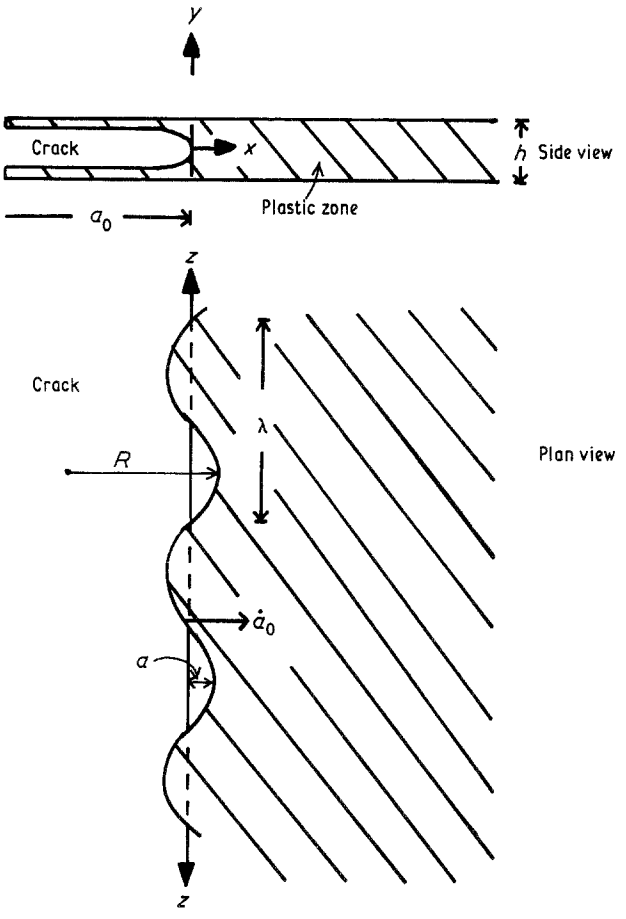

Figure 5 Schematic model of meniscus instability mechanism.

energy required to solely rupture primary and secondary bonds in extending the crack by unit area. Thus

$$\left(\frac{dp}{dx}\right)_0 a > \frac{G_0}{R} \tag{5}$$

and the minimum wavelength, λ_m, for a perturbation to grow is, by substituting from Equation 4

$$\left(\frac{dp}{dx}\right)_0 = \frac{4\pi^2 G_0}{\lambda_m^2}, \tag{6}$$

therefore

$$\lambda_m = 2\pi \left[\frac{G_0}{(dp/dx)_0}\right]^{1/2} \tag{7}$$

Now plastic flow in polymers is non-Newtonian and may be described by a power-law equation of the form

$$\left(\frac{\dot{e}}{\dot{e}_0}\right) = \left(\frac{\sigma_y}{\sigma_{y0}}\right)^n \tag{8}$$

where σ_y is the tensile yield stress at a strain rate, $\dot{e}$, and σ_{y0}, $\dot{e}_{y0}$ and n are material constants ($n = 1$ for Newtonian flow and $n = \infty$ for perfectly plastic flow). For a material with this type of flow law Fields and Ashby [10] and Argon and Salama [11] have computed

$$\left(\frac{dp}{dx}\right) = \frac{2\sigma_{y0}}{3^{1/2}h}\left(\frac{2(n+2)\dot{a}_0}{3^{1/2}\dot{e}_0 h}\right)^{1/n} \tag{9}$$

where $\dot{a}_0$ is the crack velocity and h is the thickness of the plastic zone. Thus substituting from Equation 9 into Equation 7, gives

$$\lambda_m = 2\pi\left(\frac{3^{1/2}hG_0}{2\sigma_{y0}}\right)^{1/2}\left[\frac{3^{1/2}\dot{e}_0 h}{2(n+2)\dot{a}_0}\right]^{1/2n} \tag{10}$$

Now this equation represents the minimum wavelength which will just grow and the value of λ which grows most rapidly, λ_c, is simply [10, 11]

$$\lambda_c = 3^{1/2}2\pi\left(\frac{3^{1/2}hG_0}{2\sigma_{y0}}\right)^{1/2}\left(\frac{3^{1/2}\dot{e}_0 h}{2(n+2)\dot{a}_0}\right)^{1/2n} \quad (11)$$

Hence, the wavelength of the finger-like instabilities growing ahead of the main crack front may be deduced from the basic material parameters and the theoretical values of λ_c calculated from Equation 11 compared to the experimentally measured values.

4.3. Comparison between theory and experiment

Firstly, the qualitative model of a crack growing through a plastic zone forming ahead of the tip is in accord with experimental observations. In the rubber-modified epoxy a stress-whitened zone clearly forms ahead of the advancing main crack front, and the crack propagates through this zone. Furthermore, the scanning electron micrographs clearly show finger-like furrows. These features are consistent with the crack front breaking-up as the crack grows through the plastic zone, which is constrained by the elastically deformed material outside the plastic zone.

Secondly, in the case of the rubber-modified epoxy, quantitative comparisons between theory and experiment may be undertaken. (For the unmodified epoxy polymer, when ductile crack growth occurs, the assumptions of linear elastic fracture mechanics are completely invalid and so quantitative calculations of the plastic zone size are not possible.)

Considering the parameters in Equation 11, then the value of the intrinsic fracture energy, G_0, may be taken to be 0.5 J m^{-2} for the rupture of primary bonds, as is necessary in crosslinked, thermosetting polymers [1, 14]. It is possible to calculate the thickness of the plastic zone, h, using fracture mechanics. This is given by

$$h = 2r_y = \frac{1}{\pi}\left(\frac{K_{Ic}}{\sigma_y}\right)^2 \quad (12)$$

Taking a test temperature of 60° C and a rate of 1.67×10^{-5} m sec^{-1}, then a value of K_{Ic} of 3.5 MN m$^{-3/2}$ may be deduced from Fig. 1. Following previous practice [3] an appropriate value of the tensile yield stress, σ_y, may be deduced by taking an equivalent strain-rate and assuming the ratio of tensile to compressive yield stress ($\sigma_y : \sigma_{yc}$) is 0.75. This results in a value of tensile yield stress, σ_y, of 34 MPa and hence the value of h is 3.4×10^{-3} m. The tensile yield stress at 60° C is shown as a function of strain rate at 60° C in Fig. 6, having converted the data to tensile yield stresses, as described above. Using Equation 8, the values of n and $\log_{10}(\dot{e}_0/\sigma_{y0}^n)$ are 25 and -42.2, respectively. Finally, the increase in crack length is shown as a function of time at a test temperature of 60° C and a crosshead displacement rate of 1.67×10^{-5} m sec^{-1} in Fig. 7. A linear plot is obtained which gives a crack velocity, $\dot{a}_0$, of 4.2×10^{-6} m sec^{-1}. From these values Equation 11 may be employed to yield a value of the critical wavelength, λ_c, of the finger-like instabilities of 60 μm.

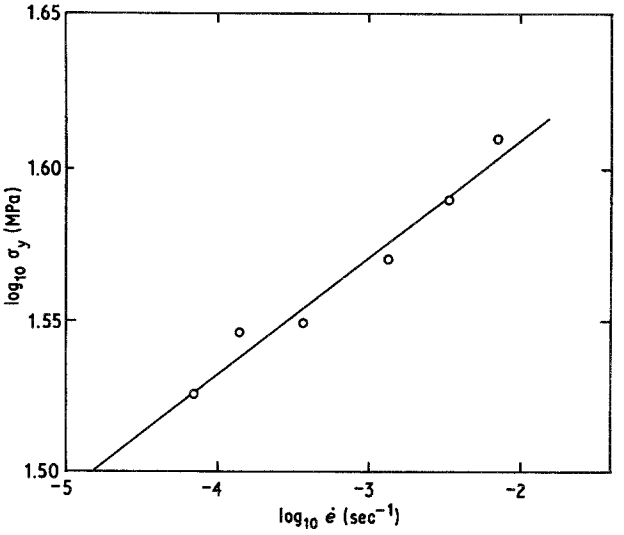

Figure 6 True tensile yield stress, σ_y, as a function of strain-rate, $\dot{e}$, at 60° C for the rubber-modified epoxy.

The experimentally determined value of λ_c from the micrographs shown in Figs. 2b and c and 3, is 68 ± 24 μm. Therefore, the theoretical model of meniscus instability is in good agreement with the experimental measurements, as well as qualitatively accounting for the observed fracture surface features.

5. Conclusions

The ductile, stable mode of crack propagation in unmodified and rubber-modified epoxy polymers that occurs at relatively high test temperatures and/or slow test rates possesses a very distinctive fracture surface consisting of finger-like furrows. These may be qualitatively explained by the suggestion that ductile stable crack growth occurs by a meniscus instability mechanism. This mechanism considers the advance of the crack front (the meniscus) through the plastic zone (modelled as a non-Newtonian fluid) formed ahead of the advancing crack, where the plastic zone is constrained by the eleastically deformed polymer which surrounds the plastic zone. Under certain conditions the smooth crack front will break-up into a series of fingers which advance ahead of the general crack front. For the rubber-modified epoxy quantitative calculations of the critical wavelength for the formation

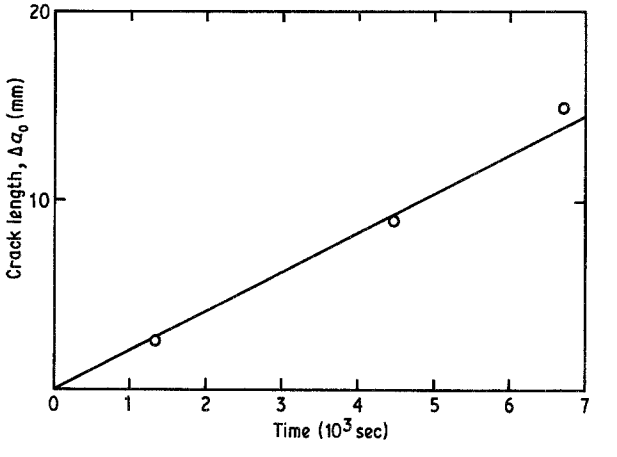

Figure 7 Crack length, Δa_0, plotted against time for ductile stable crack growth in a rubber-modified epoxy polymer (test temperature: 60° C; test rate, $\dot{y}$: 1.67×10^{-5} m sec^{-1}).

of the finger-like instabilites have been possible. The agreement between the theoretical model and experimental measurements is very good, giving support to the proposed mechanism of ductile crack growth.

References

1. A. J. KINLOCH and R. J. YOUNG, in "Fracture Behaviour of Polymers" (Applied Science, London, 1983) p. 421.
2. A. J. KINLOCH, S. J. SHAW, D. A. TOD and D. L. HUNSTON, *Polymer* **24** (1983) 1341.
3. A. J. KINLOCH, S. J. SHAW and D. L. HUNSTON, *ibid.* **24** (1983) 1355.
4. A. J. KINLOCH and J. G. WILLIAMS, *J. Mater. Sci.* **15** (1980) 987.
5. B. W. CHERRY and K. W. THOMSON, *ibid.* **16** (1981) 1925.
6. S. YAMINI and R. J. YOUNG, *ibid.* **15** (1980) 1823.
7. G. I. TAYLOR, *Proc. R. Soc.* **A201** (1950) 192.
8. P. G. SAFFMAN and G. I. TAYLOR, *ibid.* **A245** (1958) 312.
9. C. A. PAMPILLO, *J. Mater. Sci.* **10** (1975) 1194.
10. R. J. FIELDS and M. F. ASHBY, *Phil. Mag.* **33** (1976) 33.
11. A. S. ARGON and M. M. SALAMA, *Mater. Sci. Eng.* **23** (1976) 219.
12. *Idem, Phil. Mag.* **36** (1977) 1217.
13. A. M. DONALD and E. J. KRAMER, *ibid.* **43** (1981) 857.
14. J. P. BERRY, *J. Polym. Sci.* **50** (1961) 107.

Received 12 April
and accepted 30 May 1985